Delft University of Technology

Delft Center for Systems and Control

Technical report 07-033

A Hamiltonian approach for the optimal control of the switching signal for a DC-DC converter*

D. Corona, J. Buisson, and B. De Schutter

If you want to cite this report, please use the following reference instead:
D. Corona, J. Buisson, and B. De Schutter, "A Hamiltonian approach for the optimal control of the switching signal for a DC-DC converter," *Proceedings of the 17th IFAC World Congress*, Seoul, Korea, pp. 7654–7659, July 2008.

Delft Center for Systems and Control
Delft University of Technology
Mekelweg 2, 2628 CD Delft
The Netherlands
phone: +31-15-278.24.73 (secretary)
URL: `https://www.dcsc.tudelft.nl`

*This report can also be downloaded via `https://pub.deschutter.info/abs/07_033.html`

A Hamiltonian approach for the optimal control of the switching signal for a DC-DC converter ⋆

Daniele Corona * **Jean Buisson** ** **Bart De Schutter** ***

* *Delft Center for Systems and Control, Delft University of Technology, Delft, The Netherlands. (d.corona@tudelft.nl).*
** *Supélec-IETR, Cesson-Sévigné, Rennes, France. (jean.buisson@supelec.fr).*
*** *Delft Center for Systems and Control and Marine and Transport Technology department, Delft University of Technology, Delft, The Netherlands.(b@deschutter.info).*

Abstract: The optimal control problem of a switching DC-DC converter is considered in this paper. An LQ (Linear Quadratic) type performance index of the error between the current state variables and the target working point is defined. The feedback control on the decision variable of the duty cycle frequency is then formulated as a minimization of an appropriate Hamiltonian function of which suboptimal solutions are proposed. These are based on a detailed study of the average model of the system, obtained from the desired steady state solution. This paper focuses on a particular converter (the Buck-Boost converter), but the results are easily extensible to all single switch-cell converters.

Keywords: Control of switched systems; Non-smooth and discontinuous optimal control problems; Industrial applications of optimal control.

1. INTRODUCTION

Power converters are widely used in industry, and in particular in variable speed DC motor drives, computer power supplies, cell phones, and cameras. They are electrical circuits controlled by switches (transistors, diodes), used to adapt the energy supplied by a power source to a load. A notable subclass of power converter is the DC-DC converter, which aims to supply to a generic load a constant voltage/current level. Aiming at reducing switching losses and EMI (Electromagnetic Interference) of power converters a lot of soft switching techniques are developed to trade off high efficiency with commercial needs. These circuits are designed so that the switching action does not provoke discontinuity in nominal conditions.

Several control techniques and stability analysis have been proposed in literature for the DC-DC converters. Relevant practical applications use Pulse-Width-Modulation (PWM), which relies on the approximation of the switching behavior of the converter with a continuous averaged model (Lehman and Bass, 1996). An average model may be obtained by numerical or symbolic appropriate packages (Sun and Grotstollen, 1997). Continuous control approaches are then used, among which passivity-based control (Sira-Ramirez, 1991) and sliding mode control (Sira-Ramirez, 1987; Tan et al., 2006). The implementation of a fuzzy controller is studied in Gupta et al. (1997), where the authors analyze the difficulties of the real-time operation of the converter. A stability analysis for the single inductor DC-DC converter is carried out by Benadero et al. (2006). In that paper the authors analyze the stability in terms of power stage and control parameters in a PWM converter with a double proportional integral feedback. It is also relevant to consider the stability conditions for a multi-converter power system (like cars, air and space craft, submarines), as in Del Ferraro and Capponi (2005).

Recently these devices have been studied within the hybrid modeling framework and in particular they are cast in the subclass of switched systems (without jumps), which have received significant attention in the last decades (Sun and Ge, 2005; Liberzon, 2003). A control technique, based on the study of a common Lyapunov function for the switched system, can be found in Buisson et al. (2005). In addition, optimal control strategies have been used by Geyer et al. (2004); another possible approach, based on dynamic programming, is used in Corona et al. (2007) to achieve regulation by means of an LQ type cost function minimization. A vast analysis of optimal-control-based approaches for the switching power converters appears in Midya and Krein (1992), where the performance index used is the quadratic error to the target trajectory, and an initial investigation of the switching behavior is tackled. The LQR (linear quadratic regulator) scheme, parameterized in terms of the sole decision variable of the duty cycle ratio, has been studied by Fujioka et al. (2007), where the linear quadratic cost function approximates the nonlinearities emerging from the inter-sampling behavior. Regarding the control problem as an LQR offers also the advantage of being general to all PWM types of switching DC-DC converters (Leung et al., 1991).

In this paper we attempt to derive analytically the switching manifold of the converter that optimally stabilizes the state $\bar{x} = [i, v]^{\mathrm{T}}$ to a desired working point $\bar{x}_{\mathrm{p}} = 0$ [1].

⋆ Research supported by the European 6th Framework Network of Excellence "HYbrid CONtrol: Taming Heterogeneity and Complexity of Networked Embedded Systems (HYCON)", contract number FP6-IST-511368, the BSIK project "Next Generation Infrastructures (NGI)", the STW project "Multi-agent control of large-scale hybrid systems" (DWV.6188), and an NWO Van Gogh grant (VGP 79-99).

[1] The choice of $\bar{x}_{\mathrm{p}} = 0$ is not restrictive; in fact it is always possible to consider a reference system centered in $\bar{x}_{\mathrm{p}}$.

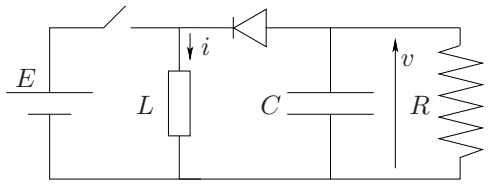

Fig. 1. *Circuit scheme of the buck-boost converter.*

The results in Corona et al. (2007) have showed that the optimal strategy consists in remaining in a particular initial mode for a given time t, and then to slide along a switching manifold $f(\bar{x}) = 0$ towards the target point $\bar{x}_{\rm p}$. From this result we show that some suboptimal strategies prove to be very efficient in terms of computational effort and accuracy ratio. We provide in Section 2 a model description for a particular application under study (the buck-boost converter). The suboptimal strategies are then described in Sections 3 and 4. Some illustrative numerical simulations are presented in Section 5.

2. MODEL DESCRIPTION

In order to derive models for DC-DC converters, different energy-based approaches, such as circuit theory, bond graphs, Euler Lagrange, Hamiltonian approach can be used. For switching systems, extensions of the Hamiltonian approach (Escobar et al., 1999), of the bond graph approach (Buisson et al., 2002) or the complementarity modeling framework (van der Schaft and Schumacher, 1998) have been proposed. In most of these systems, one physical switch is controlled (e.g. a transistor), while the other is not (e.g. a diode).

A simple circuit representation of the *ideal* buck-boost converter is depicted in Figure 1. The continuous source E has a negligible internal resistance and infinite power. No energy is lost in the inductor L nor in the capacitor C. The diode has no voltage drop in conducting mode and switches exactly at zero voltage level. In a normal operating mode of an ideal converter both the controlled and uncontrolled switches occur simultaneously.

The converter *theoretically* has four possible operating modes. We label them with the variable ρ and we denote, as in Figure 1, by v the voltage on the capacitor and by i the inductor current. The four modes are: (I) switch closed, diode blocked ($\rho = 0$), (II) switch open, diode conducting ($\rho = 1$), (III) switch open, diode blocked ($\rho = 2$), (IV) switch closed, diode conducting ($\rho = 3$).

In nominal behavior only modes (I) and (II) are involved. The nominal working area of the space state is $\mathcal{N} \equiv \{(i, v) \in \mathbb{R}^2 \, : \, i \geq 0, v \leq E\}$ depicted in Figure 2 in the dark-shaded area (right-bottom area of the Figure). The four modes are represented by the nodes of the oriented graph in Figure 3. The arcs indicate the discrete transitions from one mode to another; the controlled switches are solid lines, while the diode switches, depending on the state of the system, are represented by dashed lines.

In mode (I) the voltage source transfers energy into the inductor while, on the load side, the capacitor is feeding the load. After some time the switch is opened and the system goes to mode (II) where the energy stored in the inductor can now flow towards the load and the capacitor. Then the controller may close the switch again to mode (I) and so on. If the duration in mode (II) is protracted all the magnetic energy is transferred to the load and the buck-boost converter switches to the *discontinuous conduction* mode (III) (Hart, 1997). This state is reached when the

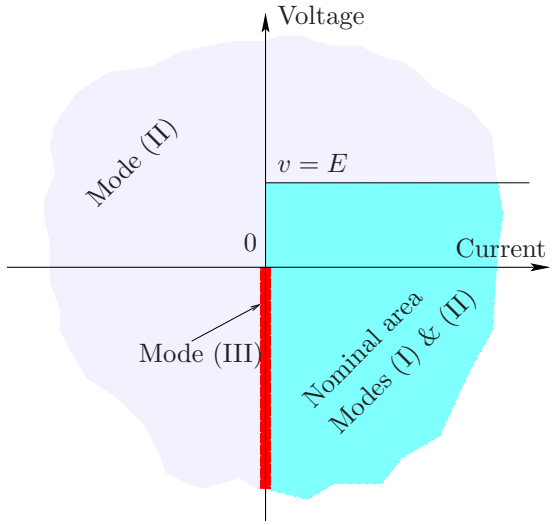

Fig. 2. *Partition of the state space for the modes of the converter.*

condition $i = 0, v < 0$ is attained. In this mode the current remains equal to zero and the capacitor is feeding the load. From (III) it is possible to switch to (I) by closing the switch.

Let us denote by $\bar{x} = [i, v]^{\rm T}$ the state. The differential equations corresponding to each location of the graph in Figure 3, are the following. In location (I) we have $\dot{\bar{x}} = \begin{bmatrix} 0 & 0 \\ 0 & -\frac{1}{RC} \end{bmatrix} \bar{x} + \begin{bmatrix} \frac{E}{L} \\ 0 \end{bmatrix}$, in location (II) $\dot{\bar{x}} = \begin{bmatrix} 0 & \frac{1}{L} \\ -\frac{1}{C} & -\frac{1}{RC} \end{bmatrix} \bar{x}$, in location (III) $\dot{\bar{x}} = \begin{bmatrix} 0 & 0 \\ 0 & -\frac{1}{RC} \end{bmatrix} \bar{x}$.

Let us observe that mode (IV) is in fact critical, because it imposes two different voltage levels in the same point (v on the anode and E on the cathode of the diode in conducting mode). If for some reason the voltage v overtakes E when the switch is closed, a *safe* controller must immediately open the switch leading to mode (II), in order to prevent harmful current peaks across the diode. Mode (IV) is, to some extent, a *fault* mode. Under this consideration the attention may be focused on a model that only contains three states and whose dynamics are given above. Furthermore, we assume that the controller of the switch is fast enough to keep the converter in the *continuous conduction* mode. This allows to disregard the third dynamics. An approach for the control of the converter in the discontinuous conduction mode requires to include guards in the model. This is a topic for future research.

The reduced modeling framework we adopt in this paper is relevant when the working point of the converter admits an *invariant region*[2] completely included in the nominal working area in Figure 2. The existence of such region is reasonable for converters composed of passive components.

These considerations lead to restrict the model in Figure 3 to the one depicted in Figure 4 with dynamics:

$$\dot{\bar{x}} = \begin{bmatrix} 0 & \frac{\rho}{L} \\ \frac{-\rho}{C} & -\frac{1}{RC} \end{bmatrix} \bar{x} + \begin{bmatrix} \frac{1-\rho}{L} E \\ 0 \end{bmatrix} = \bar{A}_\rho \bar{x} + \bar{b}_\rho, \qquad (1)$$

[2] For each initial point taken in such region there exists a controlled switching sequence that keeps the state within the invariant region.

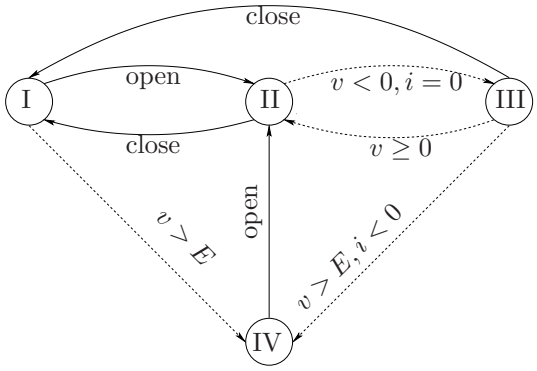

Fig. 3. *Oriented graph of the switching behavior of the converter. Solid lines: controlled switches, dashed lines: diode switches.*

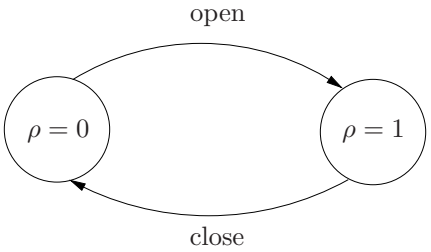

Fig. 4. *Oriented graph with only the 2 nominal operating modes.*

where $\rho \in \{0,1\}$ is the switching control signal aiming to stabilize $\bar{x}$ to an operating point $\bar{x}_{\rm p}$. In this formulation, called 'port controlled Hamiltonian with dissipation' (Buisson et al., 2005), the matrices can be expressed in the form $\bar{A}_\rho = \bar{A}_0 + (\bar{A}_1 - \bar{A}_0)\rho$ and $\bar{b}_\rho = \bar{b}_0 + (\bar{b}_1 - \bar{b}_0)\rho$.

Additionally for any given load voltage $\bar{x}_{\rm p,2}$ there exists a unique value of $\rho = \rho_{\rm m} \in [0,1]$, solution of $\bar{A}_\rho \bar{x}_{\rm p} + \bar{b}_\rho = 0$ at the equilibrium, called *average* ρ. The corresponding matrices $\bar{A}_{\rho_{\rm m}}$ and $\bar{b}_{\rho_{\rm m}}$ define the *average dynamics* of the converter. The duty cycle mode (Hart, 1997) is a specific stable limit cycle where the permanence times δ_0 and δ_1 in modes $\rho = 0$ and $\rho = 1$ respectively are constant. In this mode the average $\rho_{\rm m}$ is the ratio between δ_1 and the period of the duty cycle $\delta_0 + \delta_1$. Note that in the reference system where $\bar{x}_{\rm p} = 0$, it holds that $\bar{b}_{\rho_{\rm m}} = 0$ and that $\bar{A}_{\rho_{\rm m}}$ is a strictly Hurwitz matrix.

In a sliding mode behavior, where the switching occurs at infinite rate, the instant ratio $\rho(t) = \frac{\delta_1(t)}{\delta_0(t)+\delta_1(t)}$ is a continuous function defined in the interval $[0,1]$. For the previous consideration on the duty cycle the terminal value $\rho(+\infty)$ must converge to $\rho_{\rm m}$.

3. PROBLEM DEFINITION

In a previous paper (Corona et al., 2007) the switching control signal ρ was obtained by applying to the described model a procedure based on optimal control and dynamic programming. The results proved that the optimal solution consists of two terms. One is a transient term in the initial mode $\rho(0)$ until the state x hits a sliding surface $f(x) = 0$. The other term corresponds to the evolution along the sliding surface, switching at infinitely high rate between the two nominal modes. The objective of this paper is to investigate alternative ways to compute this optimal sliding surface. Some suboptimal solutions at reduced time and computation efforts are also proposed.

Without loss of generality it is more convenient to consider the modeling of the affine system (1) in the augmented state space. Therefore, an additional dummy variable x_n can be added to the space $\bar{x}$ so that the new state space is $x = [\bar{x}^{\rm T}, x_n]^{\rm T}$, with $x_n(0) = 1$. In this augmented state space, the evolution is described by the autonomous differential equation $\dot{x} = A_\rho x$, where $A_\rho = A_0 + (A_1 - A_0)\rho$ and $A_\rho = \begin{bmatrix} \bar{A}_\rho & \bar{b}_\rho \\ 0 & 0 \end{bmatrix}$. In order to identify the sliding surface $f(x) = 0$, the solution of the following problem is searched. Given an initial point $(x(0), \rho(0))$ solve:

$$J(x(0),\rho(0)) = \min_{\rho(t)\in[0,1]} \int_0^\infty x^{\rm T} Q_{\rho(\tau)} x d\tau \quad \text{s.t. } \dot{x} = A_{\rho(t)} x, \tag{2}$$

with $Q_\rho = \begin{bmatrix} \bar{Q}_\rho & 0 \\ 0 & 0 \end{bmatrix}$, $\bar{Q}_\rho = \bar{Q}_0 + (\bar{Q}_1 - \bar{Q}_0)\rho$, and $\bar{Q}_0 > 0$, $\bar{Q}_1 > 0$. Being $A_\rho = A_0 + (A_1 - A_0)\rho$, this nonlinear optimal control problem may be tackled by means of the Pontryagin maximum principle. This requires the introduction of the Hamiltonian function

$$H(x,p,\rho,t) \triangleq x^{\rm T} Q_\rho x + p^{\rm T} A_\rho x. \tag{3}$$

If the function $\rho(t)$ is extremal for the functional (2), then it satisfies the following necessary conditions (Kirk, 1970):

$$\begin{cases} \dot{x} = \dfrac{\partial H}{\partial p} = A_{\rho(t)} x \\ \dot{p} = -\dfrac{\partial H}{\partial x} = -A_{\rho(t)}^{\rm T} p - 2 Q_{\rho(t)} x \\ 0 = \dfrac{\partial H}{\partial \rho} = x^{\rm T}(Q_1 - Q_0)x + p^{\rm T}(A_1 - A_0)x, \end{cases} \tag{4}$$

where the function $\rho(t)$ has boundary conditions $\rho(0) \in \{0,1\}$ and $\rho(\infty) = \rho_{\rm m}$. Additionally, being the expected solution bounded by the admitted values for $\rho(t)$ (i.e., $\rho(t) \in [0,1]$), the solution of the problem has the following structure:

$$\rho^* = \begin{cases} 0 & \text{if } x^{\rm T}(Q_1 - Q_0)x + p^{\rm T}(A_1 - A_0)x > 0 \\ 1 & \text{if } x^{\rm T}(Q_1 - Q_0)x + p^{\rm T}(A_1 - A_0)x < 0 \\ \rho^*(t) & \text{if } x^{\rm T}(Q_1 - Q_0)x + p^{\rm T}(A_1 - A_0)x = 0, \end{cases} \tag{5}$$

where $\rho^*(t)$ is the solution of the Hamiltonian system (4). The first two terms of (5) certify that the minimum value of the Hamiltonian function (3) is at the domain boundary of the decision variable ρ.

4. PROPOSED SOLUTION

The description given above requires the solution of system (4), which is not straightforward. Moreover, the solution is not necessarily state feedback. Knowing that the switching rate converges to $\rho_{\rm m}$ (Section 2), the following suboptimal problem with only one switch is tackled:

$$J(x(0)) = \min_{\substack{T\geq 0 \\ \rho(0)\in\{0,1\}}} \int_0^\infty x^{\rm T} Q_{\rho(t)} x dt \quad \text{s.t. } \dot{x} = A_{\rho(t)} x, \quad \rho(t) = \begin{cases} \rho(0) & \text{if } t \in [0,T] \\ \rho_{\rm m} & \text{if } t > T \end{cases} \tag{6}$$

where $A_{\rho_{\rm m}}$ is the matrix of the average dynamics.

For each initial condition $x(0)$ the problem above gives the value of the time T^* after which a switch to the average model occurs, and such that it minimizes the criterion. The

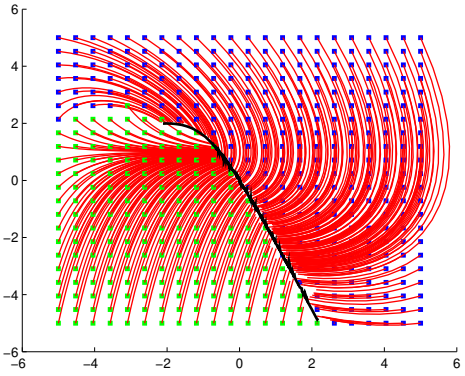

Fig. 5. *Solution of problem* (6). *In green (left-bottom) the model* $\rho = 0$ *and in blue (top-right)* $\rho = 1$, *and their corresponding trajectories in red.*

numerical result of problem (6) is depicted in Figure 5. In order to locate its minimum we solve:

$$\frac{\partial J(x(0),\rho(0),T)}{\partial T} = 0, \tag{7}$$

where

$$J(x(0),\rho(0),T) = \int_0^\infty x^{\mathrm{T}} Q_{\rho(t)} x dt$$
$$\text{s.t.} \quad \dot{x} = A_{\rho(t)} x \tag{8}$$
$$\rho(t) = \begin{cases} \rho(0) & \text{if } t \in [0,T] \\ \rho_{\mathrm{m}} & \text{if } t > T. \end{cases}$$

After some simple steps detailed in Appendix A, we get the quadratic form

$$f(x(0),\rho(0),T^*) = x(0)^{\mathrm{T}} \big(e^{A_{\rho(0)}^{\mathrm{T}} T^*} Q_{\rho(0)} e^{A_{\rho(0)} T^*} + A_{\rho(0)}^{\mathrm{T}} e^{A_{\rho(0)}^{\mathrm{T}} T^*} P e^{A_{\rho(0)} T^*} + e^{A_{\rho(0)}^{\mathrm{T}} T^*} P A_{\rho(0)} e^{A_{\rho(0)} T^*} \big) x(0) = 0, \tag{9}$$

where $P = \begin{bmatrix} \bar{P} & 0 \\ 0 & 0 \end{bmatrix}$ and $\bar{P}$ is the unique solution of the Lyapunov equation

$$\bar{A}_{\rho_{\mathrm{m}}}^{\mathrm{T}} \bar{P} + \bar{P} \bar{A}_{\rho_{\mathrm{m}}} = -\bar{Q}_{\rho_{\mathrm{m}}} \tag{10}$$

of the average model.

Assuming that there exists a *common* sliding surface[3] X this surface will not depend on the initial mode $\rho(0)$ and it is the set of points such that $T^* = 0$, solution of problem (6). Hence $X \equiv \{x : f(x,\rho,0) = 0, \forall \rho\}$. Under these considerations (9) becomes

$$f_0(x,0,0) = x^{\mathrm{T}} \big(Q_{\rho_{\mathrm{m}}} + A_0^{\mathrm{T}} P + P A_0 \big) x = x^{\mathrm{T}} F_0 x = 0, \tag{11}$$

when $\rho(0) = 0$ or

$$f_1(x,1,0) = x^{\mathrm{T}} \big(Q_{\rho_{\mathrm{m}}} + A_1^{\mathrm{T}} P + P A_1 \big) x = x^{\mathrm{T}} F_1 x = 0, \tag{12}$$

when $\rho(0) = 1$.

To complete this computation we now show that the sets $X_0 \equiv \{x : x^{\mathrm{T}} F_0 x = 0\}$ and $X_1 \equiv \{x : x^{\mathrm{T}} F_1 x = 0\}$ are equal. To this purpose we will prove the following property.

[3] This assumption is not restrictive, in fact the power converters with one commutation cell (like the Buck, the Boost, and the Čuk converter) admit a limit cycle behavior around the desired equilibrium point (Hart, 1997). When the period of this cycle goes to 0, the behavior can be interpreted as a sliding mode. From a geometrical point of view it corresponds to the presence of an attractive switching surface between the two modes.

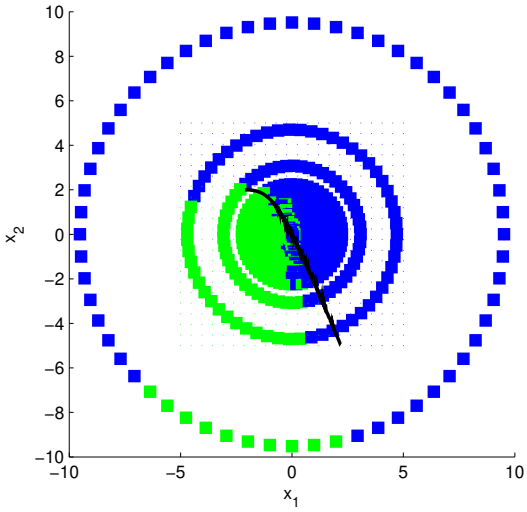

Fig. 6. *Juxtaposition of the result in Corona et al. (2007) with the switching law obtained with the approximated criterion* (6). *The right and dark zone corresponds to* $\rho = 1$, *and the left and light zone to* $\rho = 0$.

Property 4.1. The switching surfaces described by (11) and (12) are identical and they are independent from $\rho(0)$.

Proof. Let us define

$$F(\rho) = Q_\rho + A_\rho^{\mathrm{T}} P + P A_\rho, \tag{13}$$

with $A_\rho = A_0 + (A_1 - A_0)\rho$ and $Q_\rho = Q_0 + (Q_1 - Q_0)\rho$. Substituting these last two equations in (13) we obtain:

$$F(\rho) = F_0 + (F_1 - F_0)\rho. \tag{14}$$

Note that from (10) we have $Q_{\rho_{\mathrm{m}}} + A_{\rho_{\mathrm{m}}}^{\mathrm{T}} P + P A_{\rho_{\mathrm{m}}} = 0$, therefore

$$F(\rho_{\mathrm{m}}) = F_0 + (F_1 - F_0)\rho_{\mathrm{m}} = 0,$$

so

$$F_0 = -F_1 \frac{\rho_{\mathrm{m}}}{1 - \rho_{\mathrm{m}}}.$$

Hence, the quadratic forms defined by (11) and (12) are equivalent, thus $X_0 \equiv X_1$ and the switching surface does not depend on the particular initial value of ρ. □

Equation (11) (or (12)) is a conic section and it is not a particular trajectory of the average model. It can also be shown that the target point $x_{\mathrm{p}} = [0,0,1]^{\mathrm{T}}$ belongs to X. The profile of this surface and the result obtained in Corona et al. (2007) by means of the STP (Switching Table Procedure) are similar, as depicted in Figure 6.

In order to obtain the feedback switching signal $\rho(x)$ along the surface we proceed as it follows: clearly, if $x^{\mathrm{T}} F x = 0$ it also holds that $\frac{d(x^{\mathrm{T}} F x)}{dt} = 0$. This implies that

$$\dot{x}^{\mathrm{T}} F x + x^{\mathrm{T}} F \dot{x} + x^{\mathrm{T}} \dot{F} x = 0. \tag{15}$$

The term $x^{\mathrm{T}} \dot{F} x$ in (15) does not contribute, since, from (14), we have $\dot{F} = \dot{\rho}(F_1 - F_0)$, and therefore $x^{\mathrm{T}} \dot{F} x = \dot{\rho} x^{\mathrm{T}} (F_1 - F_0) x = 0$, since x belongs to the sliding surface.

Inserting in (15) the state equation with a time-varying ratio of the duty cycle, $\dot{x} = A_0 x + (A_1 - A_0)\rho(t)x$, we obtain

$$\rho(x) = -\min \left\{ \max \left(\frac{x^{\mathrm{T}} M_0 x}{x^{\mathrm{T}} M_1 x}, 0 \right), 1 \right\}, \tag{16}$$

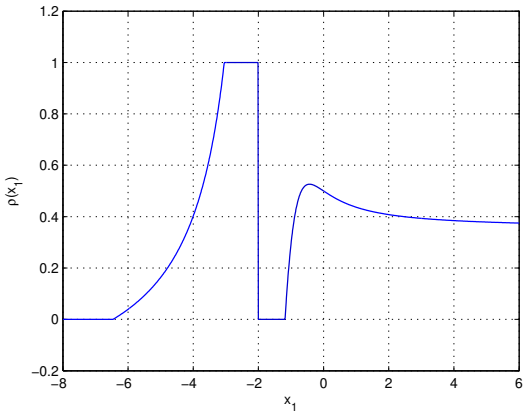

Fig. 7. *Function $\rho(x_1)$ when x is along the switching surface, for the numerical example described in Section 5.*

where $M_0 = A_0^{\mathrm{T}}F + FA_0$ and $M_1 = A_1^{\mathrm{T}}F + FA_1 - M_0$, which may be used to describe the feedback law. We depict in Figure 7 the expression of the switching signal $\rho(x)$ when the point x is moving along the switching surface.

Let us now show that the costs of the evolution along the switching surface and the cost of the evolution with the average model are the same if the initial point x belongs to the switching surface:

Property 4.2. Given a point x on the switching surface $x^{\mathrm{T}}Fx = 0$, the costs

$$\begin{aligned} J_F(x) &= \int_0^\infty x^{\mathrm{T}} Q_\rho \; x dt \\ \text{s.t.} \;& \dot{x} = A_{\rho(t)} x \\ & x(t)^{\mathrm{T}} F x(t) = 0, \end{aligned} \tag{17}$$

and

$$\begin{aligned} J_{\mathrm{m}}(x) &= \int_0^\infty x^{\mathrm{T}} Q_{\rho_{\mathrm{m}}} \; x dt \\ \text{s.t.} \;& \dot{x} = A_{\rho_{\mathrm{m}}} x, \end{aligned} \tag{18}$$

are equal.

Proof. Clearly $J_{\mathrm{m}}(x, t = \infty) = x^{\mathrm{T}}Px$, where P solves $Q_{\rho_{\mathrm{m}}} + A_{\rho_{\mathrm{m}}}^{\mathrm{T}} P + PA_{\rho_{\mathrm{m}}} = 0$. Consider a point $x + dx$ such that $(x + dx)^{\mathrm{T}}F(x + dx) = 0$, reached after a time dt of the evolution along the switching surface. We may consider the cost of an evolution that proceeds along the switching surface until $x + dx$ is reached and then switches to the average model. We have

$$J(x) = x^{\mathrm{T}} Q_\rho x dt + J_{\mathrm{m}}(x + dx, t = \infty), \tag{19}$$

which is equal to

$$J(x) = x^{\mathrm{T}} Q_\rho x dt + (x + dx)^{\mathrm{T}} P (x + dx). \tag{20}$$

In a short time interval we may consider $\rho(t) = \bar{\rho} = constant$. This allows to define $\bar{A} = A_{\bar{\rho}}$ and $\bar{Q} = Q_{\bar{\rho}}$. Being [4] $x + dx = e^{\bar{A}dt}x = (I + \bar{A}dt)x + O((dt)^2)$, (20) becomes

$$J(x) = x^{\mathrm{T}} \bar{Q} x dt + x^{\mathrm{T}} (I + \bar{A}dt)^{\mathrm{T}} P (I + \bar{A}dt) x + O((dt)^2), \tag{21}$$

which, after some steps, becomes

$$\begin{aligned} &J(x) = x^{\mathrm{T}} \bar{Q} x dt + x^{\mathrm{T}} (\bar{A}^{\mathrm{T}} P + P\bar{A}) x dt + \\ &J_{\mathrm{m}}(x) + O((dt)^2). \end{aligned} \tag{22}$$

[4] The symbol O refers to the so called big O notation: for two scalar functions f and g we have $f(t) = O(g(t))$ for $t \to 0$ if and only if there exist real numbers $\varepsilon > 0$ and $M > 0$ such that $|f(t)| \leqslant M|g(t)$ for all t with $|t| \leqslant \varepsilon$.

We show that $x^{\mathrm{T}}(\bar{Q} + \bar{A}^{\mathrm{T}}P + P\bar{A})xdt = 0$. In fact, being $\bar{Q} = Q_0 + (Q_1 - Q_0)\bar{\rho}$ and $\bar{A} = A_0 + (A_1 - A_0)\bar{\rho}$, we obtain

$$x^{\mathrm{T}}(\bar{Q} + \bar{A}^{\mathrm{T}}P + P\bar{A})x = x^{\mathrm{T}}\bar{F}x,$$

with $\bar{F} = F_0 + (F_1 - F_0)\bar{\rho}$. By hypothesis $x^{\mathrm{T}}F_0x = x^{\mathrm{T}}F_1x = 0$ (as x is on the switching surface), hence $x^{\mathrm{T}}\bar{F}x = 0$, and therefore

$$J(x) = J_{\mathrm{m}}(x) + O((dt)^2) \approx J_{\mathrm{m}}(x, t = \infty). \tag{23}$$

With similar arguments the same result may be obtained for the evolution from the point $x + dx$ and another small time increment, showing that $J_F(x) = J_{\mathrm{m}}(x)$. □

Property 4.2 shows that the evolution following the nonlinear controller described by (16) is equivalent, according to the criterion with weights Q_ρ, to the evolution that switches indefinitely fast around the average model.

Finally it is relevant to observe that if the initial point point $x(0)$ is chosen in the nominal working area, the asymptotic stability is guaranteed by the attractiveness of the switching surface and the passivity of the components.

5. NUMERICAL SIMULATIONS

In order to illustrate the results described in this paper, a numerical example, the buck-boost converter depicted in Figure 1, is considered. The numerical values of the physical system are normalized, hence $E = 1$, $L = 1$, $C = 1$ and $R = 1$. We select the set-point $\bar{x}_{\mathrm{p}} = [2, -1]^{\mathrm{T}}$, to which corresponds the average model $\rho_{\mathrm{m}} = 0.5$. Three different optimal controllers are studied.

The first controller consists in using the suboptimal switching manifold derived in Section 4. In particular, we have implemented the state feedback solution of equation (16), depicted in Figure 7. Note that this nonlinear controller uses a time-varying ratio of the duty cycle ρ, according to (16).

The second controller consists in using the initial given mode until the state space hits the optimal switching surface. From there on the system evolves with a constant duty cycle ratio corresponding to the average model.

Note that in force of Property 4.2 these first two controllers are equivalent in terms of performance index.

Finally we have implemented the optimal controller derived in Corona et al. (2007), for completeness reported in Figure 6.

For these three different controllers we have chosen 11 *significant* initial points. These points are significant because they force the controllers to work in areas of the state space where the resolution is not numerically accurate, or where we expect that further theoretical results should be pioneered. In Table 1 the values of the costs are listed for these 11 significant initial points for the mentioned three different cases: (I) Evolution with (16); (II) Evolution with (6); (III) Evolution with the law depicted in Figure 6.

The results obtained from these numerical experiences deserve some comments. First it is remarkable to observe that, for each considered initial point, the performance of the suboptimal controllers is competitive with the optimal one. The minor differences may be due to the numerical inaccuracy of the control law in Figure 6. This implies that an (almost) optimal switching signal for this converter (still easily extensible to other converters) can be obtained by means of simple analytical calculations.

Table 1. *Costs of the evolution for three different control techniques.*

x	-5	-5	5	5	2.62	-1.19	0.24	-5	-2.14	-1.19	-4.05
	-5	5	-5	5	2.62	-1.67	-3.57	2.14	2.62	-2.14	-2.14
J_F	52.93	36.40	34.46	58.84	11.99	1.28	5.77	44.63	8.81	3.55	30.14
J_{m}	52.94	36.41	34.47	58.85	12.00	1.28	5.77	45.62	8.93	3.55	29.25
J^*	53.60	36.61	32.89	58.26	11.94	1.36	5.64	49.98	9.08	3.75	30.13

6. CONCLUSION

An optimal control problem for the design of a feedback switching signal for a DC-DC converter has been studied. The performance index, based on the quadratic error between the state and the target working point, offers the possibility of designing the law by means of minimization of a Hamiltonian function. In addition, suboptimal solution have been developed and compared with the result in Corona et al. (2007).

For future research it would be interesting to investigate and quantify the error of the suboptimal solution with the optimal one obtained in Corona et al. (2007). Specific further analysis on the suboptimal solution should study the sign of the second derivative of J defined in (8), to obtain additional constraints on the switching manifold. Additional design requirements can be imposed on the controller in order to prevent potential risk of instability due to high frequency switching.

REFERENCES

L. Benadero, R. Giral, A. El Aroudi, and J. Calvente. Stability analysis of a single inductor dual switching DC-DC converter. *Mathematics and Computers in Simulation*, 71(4-6):256–269, 2006.

J. Buisson, H. Cormerais, and P.Y. Richard. Analysis of the bond graph model of hybrid physical systems with ideal switches. *Journal of Systems and Control Engineering*, 216:47–72, 2002.

J. Buisson, P.Y. Richard, and H. Cormerais. On the stabilisation of switching electrical power converters. In *Hybrid Systems: Computation and Control*, number 3414 in LNCS, pages 184–197, Zürich, Switzerland, 2005. Springer Verlag.

D. Corona, J. Buisson, B. De Schutter, and A. Giua. Stabilization of switched affine systems: an application to the buck-boost converter. In *Proc. IEEE American Control Conf.*, New York, USA, July 2007.

L. Del Ferraro and F.G. Capponi. Stability conditions for multi-converter power systems. In *Proc. IEEE Conf. Vehicle power and propulsion*, pages 137–142, Chicago, USA, September 2005.

G. Escobar, A. van der Schaft, and R. Ortega. A Hamiltonian viewpoint in the modeling of switching power converters. *Automatica*, 35(3):445–452, 1999.

H. Fujioka, C.Y. Kao, S. Almér, and U. Jönsson. LQ optimal control for a class of pulse width modulated systems. *Automatica*, 43(6):1009–1020, 2007.

T. Geyer, G. Papafotiou, and M. Morari. On the optimal control of switch-mode dc-dc converters. *Hybrid Systems: Computation and Control*, 2993:342–356, March 2004.

T. Gupta, R.R. Boudreaux, R.M. Nelms, and J.Y. Hung. Implementation of a fuzzy controller for DC-DC converters using an inexpensive 8-b microcontroller. *IEEE Trans. Power Electronics*, 44(5):661–669, 1997.

D. Hart. *Introduction to Power Electronics*. Prentice-Hall, Upper Saddle River, New Jersey, 1997.

D.E. Kirk. *Optimal Control Theory: an Introduction*. Prentice-Hall, Englewood Cliffs, New Jersey, USA, 1970.

B. Lehman and R.M. Bass. Switching frequency dependent averaged models for PWM DC-DC converters. *IEEE Trans. Power Electronics*, 11(1):89–98, 1996.

F.H.F. Leung, P.K.S. Tam, and C.K. Li. The control of switching DC-DC converters - A general LQR problem. *IEEE Trans. Industrial Electronics*, 38(1):65–71, 1991.

D. Liberzon. *Switching in Systems and Control*. Birkhäuser, Boston, 2003.

P. Midya and P.T. Krein. Optimal control approaches to switching power converters. In *Proc. IEEE Conf. Power electronics specialists*, pages 741–748, Toledo, Spain, June 1992.

H. Sira-Ramirez. Nonlinear P-I controller design for switch-mode DC-to-DC power converters. *IEEE Trans. Circuits and Systems*, 41:499–513, 1991.

H. Sira-Ramirez. Sliding motions in bilinear switched networks. *IEEE Trans. Circuits and Systems*, 34(8): 919–933, 1987.

J. Sun and H. Grotstollen. Symbolic analysis methods for averaged modeling of switching power converters. *IEEE Trans. Power Electronics*, 12(3):537–546, 1997.

Z. Sun and S. Ge. *Switched Linear Systems*. Springer, London, 2005.

S.C. Tan, T.M. Lai, and C.K. Tse. A unified approach to the design of a PWM-based sliding mode voltage controllers for basic DC-DC converters in continuous conduction mode. *IEEE Trans. Circuits and Systems I*, 53(8):1816–1827, 2006.

A. van der Schaft and J.M. Schumacher. Complementarity modeling of hybrid systems. *IEEE Trans. Automatic Control*, 43(4):483–490, 1998.

Appendix A. CONSTRUCTION OF THE SWITCHING SURFACE

Let us consider the problem (7), where the function $J(x(0), \rho(0), t)$, detailed in (8) can be rewritten as

$$J(x(0),\rho(0),T) = \int_0^T x^{\mathrm{T}} Q_{\rho(0)} x d\tau + \int_T^\infty x^{\mathrm{T}} Q_{\rho_{\mathrm{m}}} x d\tau \quad \begin{matrix} \text{s.t. } \dot{x} = A_{\rho(0)} x \\ \text{s.t. } \dot{x} = A_{\rho_{\mathrm{m}}} x. \end{matrix} \tag{A.1}$$

By derivation over the variable T, the switching instant, we obtain

$$\frac{\partial J(x(0),\rho(0),T)}{\partial T} = x^{\mathrm{T}}(T) Q_{\rho(0)} x(T) + \frac{\partial x^{\mathrm{T}}(T) P x(T)}{\partial T},$$

which is equal to

$$\begin{aligned} \frac{\partial J(x(0),\rho(0),T)}{\partial T} &= x^{\mathrm{T}}(T) Q_{\rho(0)} x(T) + \\ & \frac{\partial x^{\mathrm{T}}(T)}{\partial T} P x(T) + x^{\mathrm{T}}(T) P \frac{\partial x(T)}{\partial T}. \end{aligned} \tag{A.2}$$

From the state equation it holds that $\frac{\partial x(T)}{\partial T} = A_{\rho(0)} x(T)$ and $x(T) = e^{A_{\rho(0)} T} x(0)$, which, substituted in (A.2), provides the analytical expression of the derivative (7),

$$\begin{aligned} \frac{\partial J(x(0),\rho(0),T)}{\partial T} &= x(0)^{\mathrm{T}} \big(e^{A_{\rho(0)}^{\mathrm{T}} T} Q_{\rho(0)} e^{A_{\rho(0)} T} + \\ & A_{\rho(0)}^{\mathrm{T}} e^{A_{\rho(0)}^{\mathrm{T}} T} P e^{A_{\rho(0)} T} + e^{A_{\rho(0)}^{\mathrm{T}} T} P A_{\rho(0)} e^{A_{\rho(0)} T} \big) x(0). \end{aligned}$$